

V-shaped dislocations in a GaN epitaxial layer on GaN substrate

Cite as: AIP Advances 9, 095002 (2019); doi: 10.1063/1.5114866

Submitted: 12 June 2019 • Accepted: 22 August 2019 •

Published Online: 5 September 2019



Atsushi Tanaka,^{1,2,a)} Kentaro Nagamatsu,³ Shigeyoshi Usami,⁴ Maki Kushimoto,⁴ Manato Deki,¹ Shugo Nitta,¹ Yoshio Honda,¹ Michal Bockowski,⁵ and Hiroshi Amano^{1,2,6,7}

AFFILIATIONS

¹Institute of Materials and Systems for Sustainability, Nagoya University, Furo-cho, Chikusa-ku 464-8601, Nagoya, Japan

²National Institute for Materials Science, 1-1, Namiki, 305-0044 Tsukuba, Japan

³Institute of Post-LED Photonics, Tokushima University, 2-1 Minami-Josanjima, 770-8506 Tokushima, Japan

⁴Department of Electrical Engineering and Computer Science, Nagoya University, Furo-cho, Chikusa-ku 464-8603, Nagoya, Japan

⁵Institute of High Pressure Physics, Polish Academy of Sciences, Sokolowska 29/37, Warsaw 01-142, Poland

⁶Akasaka Research Center, Nagoya University, Furo-cho, Chikusa-ku 464-8603, Nagoya, Japan

⁷Venture Business Laboratory, Nagoya University, Furo-cho, Chikusa-ku 464-8603, Nagoya, Japan

^{a)}Electronic mail: a_tanaka@nuee.nagoya-u.ac.jp

ABSTRACT

In this study, V-shaped dislocations in a GaN epitaxial layer on a free-standing GaN substrate were observed. Our investigation further revealed that the V-shaped dislocations were newly generated at the interface in the epilayer rather than propagated from the GaN substrate. V-shaped dislocations consist of two straight parts. The straight parts of the V-shaped dislocations were separated from each other in the *m*-direction and tilted toward the step-flow direction of the GaN epitaxial layer. The V-shaped dislocations are continuous single dislocations having a Burgers vector component of $1a$ and an intrinsic stacking fault between their straight parts.

© 2019 Author(s). All article content, except where otherwise noted, is licensed under a Creative Commons Attribution (CC BY) license (<http://creativecommons.org/licenses/by/4.0/>). <https://doi.org/10.1063/1.5114866>

Gallium nitride (GaN) is a promising material for applications in high-performance power devices because of its wide band gap, high critical electric field strength, and high bulk mobility.^{1–9} Recently, as the quality of GaN free-standing substrates has increased and the dislocation density has decreased,^{10–13} practical applications of vertical GaN power devices have received an increasing amount of attention. However, the dislocation density of commercially available substrates is from 10^3 to 10^7 cm⁻², meaning that it is still difficult to fabricate dislocation-free devices with a GaN substrate. Therefore, the effect of dislocations on the electric properties of vertical GaN devices has been extensively investigated.^{14–19} One primary objective is to fabricate devices on a substrate without dislocations. In this study, we investigate how dislocations propagate into an epitaxial layer from a substrate when using a low-dislocation-density substrate.

A commercially available epi-ready n-type GaN (0001) substrate²⁰ with a threading dislocation density (TDD) of 10^3 cm⁻² was

used in this study. The size of the substrate was 1 cm², and before initiating the growth of the epitaxial layer, the TDD of the substrate was verified by synchrotron X-ray topography. The substrate was cleaned by acetone, methanol, sulfuric peroxide mixture (SPM), aqua regia and HF solutions. The substrate was rinsed by deionized water, dried by nitrogen gas blow. An undoped GaN epitaxial layer was then grown on the substrate by metalorganic vapor phase epitaxy (MOVPE), in which trimethylgallium (TMGa) and ammonia (NH₃) were used as precursors and hydrogen (H₂) was the carrier gas. The epitaxial layer was grown at a temperature of 1100 °C, a pressure of 100 kPa, and a V/III ratio of 1019. The thickness of the epitaxial layer was 26 μm and the growth rate was 3.7 μm/h. Furthermore, synchrotron X-ray topography was used to observe the change of TDD. X-ray topography images were taken with a *g* vector of [1124] and a beam energy in the range of 8.26 to 8.28 keV. The penetration depth of the X-rays under these conditions was calculated to be about 5.4 μm, which was much smaller than

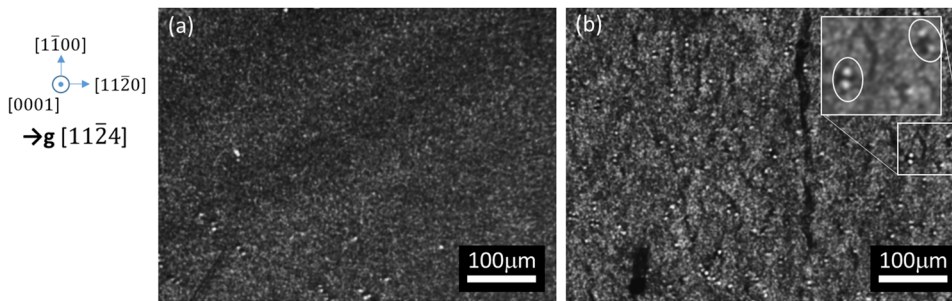


FIG. 1. X-ray topography images of (a) substrate and (b) epitaxial layer. The inset of (b) shows generated pair dislocations.

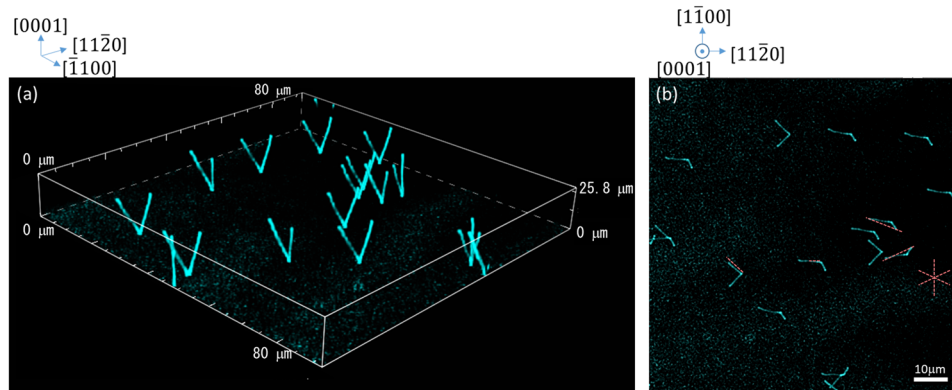


FIG. 2. MEPM images of V-shaped dislocations. (a) Three-dimensional image showing bird's-eye view. (b) Image projected onto c-plane. Dashed lines in (b) indicate the m-direction.

the thickness of the epitaxial layer. We also investigated dislocation propagation in the samples by multiphoton excitation photoluminescence microscopy (MEPM), which is an excellent tool for observing the shape of dislocations in GaN as reported in Ref. 21.

Figure 1 shows X-ray topography images of the GaN substrate before epitaxial growth (a) and the GaN epilayer after growth (b) at the same location. The TDD of the sample before epitaxial growth was $2.80 \times 10^3 \text{ cm}^{-2}$, whereas after epitaxial growth, the TDD increased to $2.21 \times 10^5 \text{ cm}^{-2}$. As shown in the inset of Fig. 1(b), dislocations typically exist in pairs, and these generated dislocations were observed throughout the sample.

Figure 2 presents MEPM images of the epitaxial layer of the sample. Dislocations are indicated as bright blue lines. Figure 2(a) is a bird's-eye view of a three-dimensional (3D) image. Figure 2(b) is a top view projected onto the c-plane. As shown in Fig. 2(a), V-shaped dislocations (VsDs) start at the interface between the epitaxial layer and the substrate. There have been several reports on the generation of VsDs during the fabrication of InGaN multiple quantum wells.^{22–24} However, there is no report about that VsDs were observed in detail in a GaN epilayer homoepitaxially grown on a GaN substrate. The red dashed lines in Fig. 2(b) indicate the m-direction. While the two linear parts of the V-shape are separated from each other in the m-direction, the VsDs separating toward $[1\bar{1}00]$ are inclined to the left-hand side in Fig. 2(b). In the cases of VsDs separating toward $[\bar{1}010]$ and $[01\bar{1}0]$, the left-hand-side portions are tilted more than the right-hand-side parts.

Observing this area by atomic force microscopy (AFM) (see Fig. 3), step-flow growth was found to occur to the left, and

it is considered that VsDs are easily tilted by a step flow. The average separating angle of dislocation was 9.5° and tilted angle towards left-hand-side was 8.6° . To obtain a detailed understanding of these VsDs, we observed one of them by high-angle annular

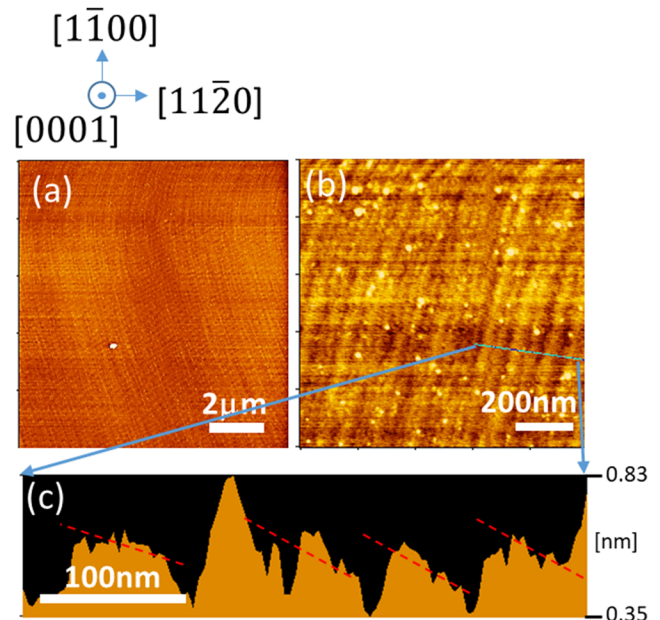


FIG. 3. AFM images of the area where MEPM observation was performed. (a) Large-area image. (b) Magnified image of (a). (c) Height profile along the line in (b). (c) indicates a steps occurred on the left-hand side of this area.

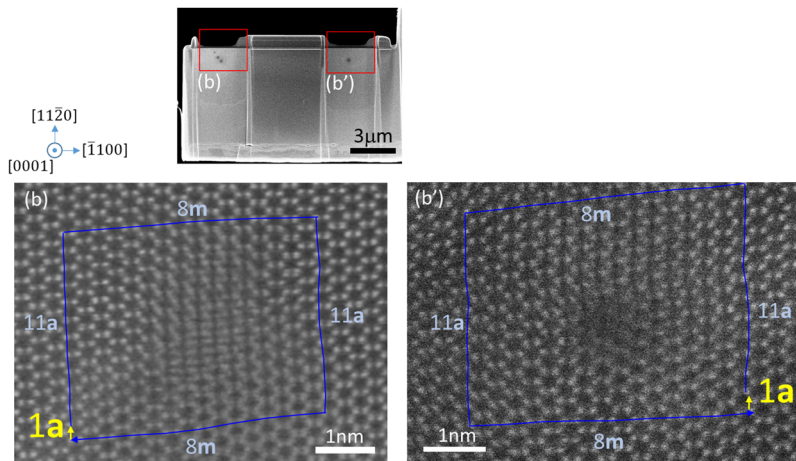


FIG. 4. SEM image of top of pair of V-shaped dislocations (a), HAADF images of each dislocation (b) and (b'). Blue lines indicate Burgers circuits and yellow arrows indicate the Burgers vectors of the dislocations enclosed in each Burgers circuit.

dark-field scanning transmission electron microscopy (HAADF-STEM). Figure 4 presents an HAADF image of the two parts of a VsD. The blue lines in Figs. 4(b) and (b') are the Burgers circuits surrounding each dislocation core, which are clockwise in Fig. 4(b) and counterclockwise in Fig. 4(b'). These Burgers circuits are drawn in such a way that the relationship between the dislocation line vector and the Burgers circuit is always constant, regarding the VsD as a single continuous dislocation. In particular, we configured the dislocation line vector to be in the backward direction in Fig. 4(b) and the forward direction in Fig. 4(b'). As shown in Figs. 4(b) and (b'), both dislocations have the same direction of the 1a edge components, which is consistent with the assumption that the VsD is a single continuous dislocation. That is, it is a newly generated half-loop dislocation. From these Burgers circuits, we can observe that there is an extra a-plane on the left-hand side of the dislocation core in Fig. 4(b) and on the right-hand side of the dislocation core in Fig. 4(b'). This means that an intrinsic stacking fault with an a-plane exists inside the VsD. Figure 5 shows schematic images of the stacking fault and the surrounding dislocation.

It is measured by XRD that this substrate has a-lattice constant of 3.1876 Å. On the other hand, it is very difficult to know ideal lattice constant of the epitaxial layer, because it is very difficult to get free-standing MOVPE layer. However, since well-known a-lattice constant of undoped GaN is 3.189 Å and the epitaxial layer is also undoped, the ideal lattice constant of the epitaxial layer must be larger than 3.1876 Å. With this assumption, generation mechanism of this VsDs can be explained in the same logic as discussed in Ref. 23 that VsDs are generated in the crystal with the larger lattice constant to produce partial stress relaxation due to the presence of an effective misfit dislocation component. Since these VsDs are affected by step-flow growth, it is natural to consider that the critical film thickness is very small and most of observed part of VsDs by MPEM in Fig. 2 are not generated from the surface but are grown with epitaxial growth. In calculating the critical film thickness, it is appropriate to assume the case without dislocation interaction, since VsDs are newly generated and no other dislocations propagated from substrate around VsDs. According to Ref. 25, critical film thickness h_c in the absence of interaction of dislocations is determined by

$$h_c \cong \left(\frac{b}{f}\right) \left[\frac{1}{4\pi(1+\nu)}\right] \left[\ln\left(\frac{h_c}{b}\right) + 1\right] \quad (1)$$

where b is the magnitude of the Burger's vector, f is the ratio of lattice mismatch, and ν is Poisson's ratio. Calculated critical film thickness is 379 nm with assuming lattice constant of epitaxial layer of 3.189 Å. This value is much less than depth direction resolution of MEPM of 3.2 μm. Therefore, the origin points of the VsD and interface of epitaxial layer and substrate can not be separated with MEPM.

The width of the intrinsic stacking faults increased with the thickness of the epitaxial layer. In other words, the 1a edge dislocation, as part of the VsD, climb towards the m-direction. For dislocation climbing, point defect is needed. In this case, since those VsDs spread during epitaxial growth, the growth surface acts as a source of point defects. About the tilting of the VsDs towards step flow

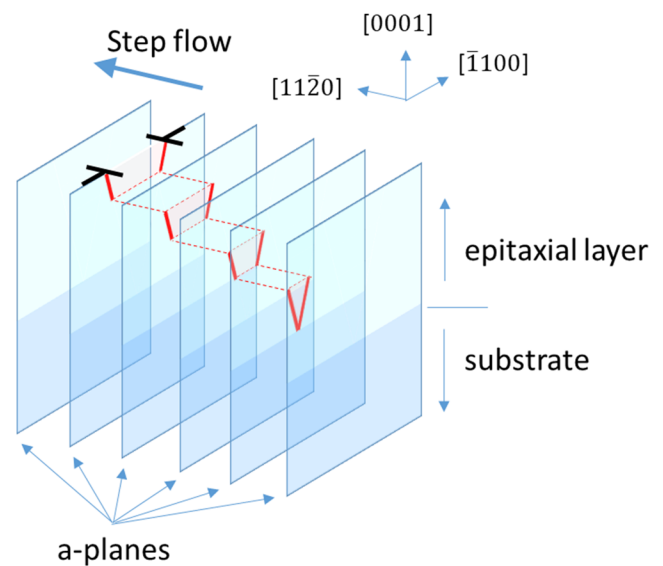


FIG. 5. Schematic images of the stacking fault and the surrounding dislocation.

direction, they have a Burgers vector of $1a$, thus, the slip plane is the m -plane and it is easy for the dislocations to tilt towards a -direction, as clearly discussed in Ref. 26.

In this study, despite the homoepitaxy, it was revealed that VsDs are generated in a GaN epitaxial layer on a GaN substrate. Lack of dislocations and difference in the lattice constant between the substrate and the epitaxial layer are considered to be a cause of generation of VsDs. Therefore, it is necessary to consider which impurity is most suitable to control the conductivity and lattice constant to suppress the generation of dislocations in an epitaxial layer of GaN on the GaN substrate with low threading dislocation density.

Part of this work was supported by MEXT, “Program for research and development of next generation semiconductor to realize energy-saving society” and JSPS KAKENHI Grant Number JP17858100.

REFERENCES

- ¹G. T. Dang, A. P. Zhang, F. Ren, X. A. Cao, S. J. Pearton, H. Cho, J. Han, J. I. Chyi, C. M. Lee, C. C. Chuo, S. N. George Chu, and R. G. Wilson, *IEEE Trans. Electron Devices* **47**, 692 (2000).
- ²Y. Yoshizumi, S. Hashimoto, T. Tanabe, and M. Kiyama, *J. Cryst. Growth* **298**, 875 (2007).
- ³K. Matocha, T. P. Chow, and R. J. Gutmann, *IEEE Trans. Electron Devices* **52**, 6 (2005).
- ⁴J. Suda, K. Yamaji, Y. Hayashi, T. Kimoto, K. Shimoyama, H. Narita, and S. Nagao, *Appl. Phys. Express* **3**, 101003 (2010).
- ⁵Z. Hu, K. Nomoto, B. Song, M. Zhu, M. Qi, M. X. Gao, V. Protasenko, D. Jena, and H. G. Xing, *Appl. Phys. Lett.* **107**, 243501 (2015).
- ⁶M. Qi, K. Nomoto, M. Zhu, Z. Hu, Y. Zhao, V. Protasenko, B. Song, G. Li, J. Verma, S. Bader, P. Fay, H. G. Xing, and D. Jena, *Appl. Phys. Lett.* **107**, 232101 (2015).
- ⁷T. Oikawa, Y. Saijo, S. Kato, T. Mishima, and T. Nakamura, *Nucl. Instrum. Methods Phys. Res. A* **365**, 168 (2015).
- ⁸A. Tanaka, K. Nagamatsu, J. Matsushita, M. Deki, Y. Ando, M. Kushimoto, S. Nitta, Y. Honda, and H. Amano, *Phys. Status Solidi A* **214**, 1600829 (2017).
- ⁹O. I. Barry, A. Tanaka, K. Nagamatsu, S. Bae, K. Lekhal, J. Matsushita, M. Deki, S. Nitta, Y. Honda, and H. Amano, *J. Cryst. Growth* **468**, 552 (2017).
- ¹⁰H. Geng, H. Sunakawa, N. Sumi, K. Yamamoto, A. A. Yamaguchi, and A. Usui, *J. Cryst. Growth* **350**, 44 (2012).
- ¹¹R. Dwiliski, R. Doradziski, J. Garczyski, L. Sierzputowski, R. Kucharski, M. Zajc, M. Rudziski, R. Kudrawiec, J. Serafczuk, and W. Strupiski, *J. Cryst. Growth* **312**, 2499 (2010).
- ¹²T. Yoshida, Y. Oshima, T. Eri, K. Ikeda, S. Yamamoto, K. Watanabe, M. Shibata, and T. Mishima, *J. Cryst. Growth* **310**, 5 (2008).
- ¹³K. Motoki, T. Okahisa, R. Hirota, S. Nakahata, K. Uematsu, and N. Matsumoto, *J. Cryst. Growth* **305**, 377 (2007).
- ¹⁴S. Usami, Y. Ando, A. Tanaka, K. Nagamatsu, M. Deki, M. Kushimoto, S. Nitta, Y. Honda, H. Amano, Y. Sugawara, Y. Z. Yao, and Y. Ishikawa, *Appl. Phys. Lett.* **112**, 182106 (2018).
- ¹⁵J. W. P. Hsu, M. J. Manfra, R. J. Molnar, B. Heying, and J. S. Speck, *Appl. Phys. Lett.* **81**, 79 (2002).
- ¹⁶K. Shiojima, T. Suemitsu, and M. Ogura, *Appl. Phys. Lett.* **78**, 3636 (2001).
- ¹⁷B. Kim, D. Moon, K. Joo, S. Oh, Y. K. Lee, Y. Park, Y. Nanishi, and E. Yoo, *Appl. Phys. Lett.* **104**, 102101 (2014).
- ¹⁸B. S. Simpkins, E. T. Yu, P. Waltereit, and J. S. Speck, *J. Appl. Phys.* **94**, 1448 (2003).
- ¹⁹J. C. Moore, J. E. Ortiz, J. Xie, H. Morkoc, and A. A. Baski, *Journal of Physics: Conference Series* **61**, 90 (2007).
- ²⁰M. Zajac, R. Kucharski, K. Grabianska, A. Gwardys-Bak, A. Puchalski, D. Wasik, E. Litwin-Staszewska, R. Piotrkowski, J. Z. Domagala, and M. Bockowski, *Prog. Cryst. Growth Charact. Mater.* **64**, 63 (2018).
- ²¹T. Tanikawa, K. Ohnishi, M. Kanoh, T. Mukai, and T. Matsuoka, *Appl. Phys. Express* **11**, 013004 (2018).
- ²²M. Zhu, S. You, T. Detchprohm, T. Paskova, E. A. Preble, D. Hanser, and C. Wetzel, *Phys. Rev. B - Condens. Matter Mater. Phys.* **81**, 125325 (2010).
- ²³A. V. Lobanova, A. L. Kolesnikova, A. E. Romanov, S. Y. Karpov, M. E. Rudinsky, and E. V. Yakovlev, *Appl. Phys. Lett.* **103**, 152106 (2013).
- ²⁴F. Y. Meng, H. McFelea, R. Datta, U. Chowdhury, C. Werkhoven, C. Arena, and S. Mahajan, *J. Appl. Phys.* **110**, 073503 (2011).
- ²⁵R. People and J. C. Bean, *Appl. Phys. Lett.* **47**, 322 (1985).
- ²⁶T. Matsubara, K. Sugimoto, S. Goubara, R. Inomoto, N. Okada, and K. Tadatomo, *J. Appl. Phys.* **120**, 185101 (2017).